Advances in Technology Innovation, vol. 10, no. 4, 2025, pp. 419-435

A Multiple-Parameter Optimization of Darrieus Vertical Axis Wind Turbine for Enhanced Performance

Dhiman Dey[1], Gour Chand Mazumder[2,*], Arnendu Roy Apu[1], Himangshu Ranjan Ghosh[1]

[1]Institute of Energy, University of Dhaka, Dhaka, Bangladesh

[2]Department of Electrical and Electronic Engineering, American International University-Bangladesh, Dhaka, Bangladesh

Received 15 June 20xx; received in revised form 05 August 20xx; accepted 10 September 20xx

DOI: https://doi.org/10.46604/aiti.2025.14914

Abstract

This paper aims to optimize a small vertical-axis wind turbine (VAWT) by analyzing chord length, hub radius, and circular angle, and establishing a relationship between design parameters and performance. The approach involves evaluating five airfoils and identifying the best airfoil using QBlade, based on comparisons of the power coefficient (C_P), tip speed ratio (TSR), and the power output (P). Mathematical relationships are developed through extrapolation using polynomial, logarithmic, and modified Avrami equations. The result shows that the 'S1046 17%' is the best-performing airfoil among the five. The optimum chord length to hub radius ratio yields the highest power output, and the impact of circular angle on performance is negligible. The Avrami equation shows better fitness to the original data than the polynomial equation. The Troposkien variant shows a higher C_P over a wide range of TSR, while the straight blade produces higher power output across varying wind speed (V).

Keywords: Avrami equation, QBlade software, vertical axis wind turbine, wind turbine optimization

1. Introduction

Wind is a form of renewable energy that is used to generate electricity using wind turbines. It is emissions-free and an environmentally friendly alternative to fossil fuels. Wind turbines are primarily of two categories: horizontal-axis wind turbines (HAWT) and vertical-axis wind turbines (VAWT). Generally, VAWTs are preferable for low-wind speed conditions [1]. Optimization is important for VAWTs to operate efficiently under low wind speed (V) conditions. VAWT can capture wind from all directions, unlike HAWT. Double helix or straight blade turbines are commonly used in a variety of shapes and orientations of blades [2]. Fig. 1 shows three types of VAWTs, each with different types of physical appearances and blade orientations. VAWTs are primarily categorized into three groups: H-Rotor, Savonius, and Darrieus. Among these, the H-Rotor and Darrieus are lift-type turbines, while the Savonius is a drag-type turbine.

The optimization of wind turbines considers maximizing energy capture, minimizing the effect of turbulence, and the impact of varying wind directions. Research focuses on enhancing the suitability of VAWTs for urban or residential areas, where wind patterns are often irregular [3]. Selecting and preparing design parameters like chord length, rotor radius, and circular angle impacts the VAWT's overall performance. Understanding the relationship between the design parameters and the performance is crucial for developing and manufacturing efficient wind turbines. Therefore, the motivation of this study is to optimize the design parameters and analyze their impact on performance to enable improved VAWT design.

This study performs a literature survey based on the recently published research articles. The survey finds that most of

* Corresponding author. E-mail address: dr.mazumder@aiub.edu

the studies focus on a narrow selection of airfoils, which constrains the evaluation of a broader range of potentially higher-performing airfoils. Additionally, the optimization technique in these studies is typically based on only one or two design parameters. Therefore, there is a need for a more comprehensive optimization approach that considers multiple parameters, such as chord length, hub radius, blade length, and circular angle. Furthermore, existing research has not attempted to establish a correlation between these design parameters and key performance indicators like the power coefficient (C_P) or tip speed ratio (TSR).

The objective of this research is to optimize a small VAWT (Darrieus Type) based on chord length, hub radius, and circular angle, and to develop a mathematical relationship between optimizing parameters and C_P. The study aims to simulate and generate data to support the analysis for a small wind turbine suitable for use in a low V region.

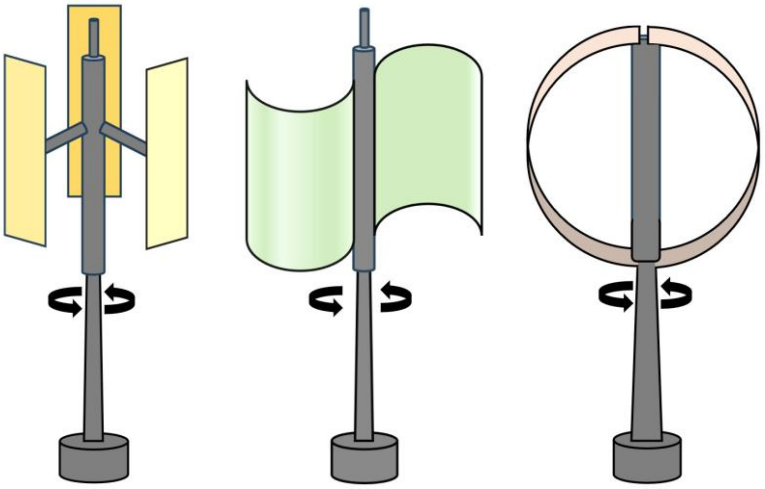

(a) H-Rotor (b) Savonius (c) Darrieus

Fig. 1 Types of VAWT

2. Literature Reviews

Muhsen et al. [4] evaluated the best-performing airfoils for designing wind turbines to operate at 4-7 m/s wind speed. They used Xfoil, MATLAB, and QBlade for airfoil selection and optimization. The designed HAWT's rotor is 4 m, has three blades, a hub height of 20 cm, a TSR of 6.5, a power generation capacity of 650W, and a C_P is 0.445 at a V of 5.5 m/s, reaching a power of 1.18 kW and a C_P of 0.40 at a V of 7 m/s. The study overlooks the impacts of circular angles on performance. It does not comment on the further reduction of rotor heights by changing other parameters.

Altmimi et al. [5] investigated a small HAWT using QBlade. The study optimizes the chord length and twist angle relating to the drag coefficient (C_D) and lift coefficient (C_L). The blade length is 1 m, and at 10 m/s V, the C_P is 0.4. The study indicates the importance of chord length as a design parameter. However, the study is limited to using only a single airfoil and examining performance relating to only two parameters.

Badah and Mahmood [6] evaluated the performance of a VAWT. They selected the Darrieus VAWT for the analysis. The study used only one airfoil and compared performance parameters like C_P, lift, and drag forces based on the number of blades, TSR, and V. The study does not explore performance based on design parameters and is limited to only a single airfoil.

Altmimi et al. [7] optimized VAWT using QBlade. The study determines the performance with respect to the environmental conditions, size, and number of blades. It optimizes the blades for a single-family airfoil based on the number of blades. However, the study does not investigate the optimization of the blade length, chord, or any angle, and also does not categorize further except by identifying it as a VAWT.

MURATOĞLU and DEMİR [8] investigated the effect of geometry and dynamic parameters on the performance of a

Darrieus turbine. The study utilizes QBlade to compare five airfoils from the National Advisory Committee for Aeronautics (NACA) family and identifies the best-performing foil. It analyzed the impact of blade numbers, chord length, and helicity angle. The study presents the C_P for a fixed height and fixed rotor size. The output power capacity is not demonstrated. The analysis may benefit from an examination of various hub heights or circular angles.

The chord length and radius of the turbine blade significantly impact the Reynolds number (Re), which thus affects the performance of power production [9]. The twist and circular angle of VAWT blades define the orientation of the blade relative to its mountings, thereby influencing the angle of attack (AoA). These parameters could significantly impact the turbine's performance [10]. Therefore, it is important to evaluate the performance due to the changes in these three parameters.

Bouanani et al. [11] used QBlade to model VAWT employing three different NACA foil profiles for the analysis. The study determined the better-performing airfoil and investigated the H rotor and Troposkien by comparing C_P, concluding that the Troposkien variant is better performing. The study did not explore the optimization possibility based on physical parameters at all.

Zhang et al. [12] conducted an experimental study on straight-bladed VAWT using QBlade. They used a 4-bladed turbine and various installation angles of the blade to assess the impact of various installation angles and optimization. The study also used three airfoils from the NACA family. Two specific hub radii are tested for the performance. The study could benefit by relating the relationship of the design parameters and might consider circular angles in the optimization process.

Davari et al. [13] performed a numerical and experimental investigation of Darrieus VAWT. The study explores the self-starting of the VAWT at low V. It uses NACA0015 and Selig airfoils with the advanced double multiple stream tube (DMST) method in MATLAB for analysis. It investigates the impact of the smooth skin and embossed surface of the turbine blade practically. It concludes that the modified NACA with embossed skin performs better among its four modes of operation while optimizing C_P upon thickness to camber ratio. However, the study is limited to only two types of airfoils and straight blade orientation.

Davari et al. [14] investigated the Blade height impact on self-starting torque for the Darrieus VAWT. The study uses DMST and particle swarm optimization methods for the optimization process. The study uses three NACA family rotors for analysis. The study concludes that the roughness of blade skin achieved by embossing with increased blade height decreases the self-starting torque for the modified NACA0015 rotor. The study investigates three airfoils of one family and examines only one physical parameter, i.e., blade height with rough and smooth surfaces.

Davari et al. [15] explored the aerodynamic efficiency by altering the geometry of the airfoil. The study takes the thickness to camber ratio as the regulating parameter with the range of Re between 50,000 and 500,000. The study takes three different airfoils and modifies the shapes for optimization. It investigates the airfoil performance parameters like C_L, C_D, and AoA. The study concludes that modification of airfoils upon the thickness-to-camber ratio improves airfoil performance for small wind turbines. The study does not exclusively mention the type of suitable small wind turbine and is limited to investigating airfoil performance, rather than the overall turbine performance using the optimized airfoil.

Davari et al. [16] conducted a study to enhance the aerodynamic efficiency of 3 airfoils from two families using QBlade software. The study changes the thickness-to-camber ratio for the modification of the base airfoils. It analyzes the performance parameters like C_D, C_L, AoA, and C_P over the range of Re between 50,000 and 500,000. The study concludes that modifying the shape can improve the airfoil performance by nearly 50%. However, the study is limited to analyzing only a small 3-bladed HAWT to investigate C_P.

Davari et al. [17] conducted a study to maximize the lift-to-drag ratio (C_L/C_D). The study exploits three airfoils from

different families and changes the thickness-to-camber ratio to modify the airfoils and generate data using XFOIL software. The study provides data on performance within the Re range between 50,000 and 100,000. The study concludes that the C_L/C_D notably improves when modified over the thickness-to-camber ratio. However, the study only investigates the C_L/C_D as the performance parameter. It only investigates airfoil performance rather than providing an analysis for wind turbine performance using optimized airfoils.

In summary, Davari et al. [13-17] have recently published five research papers, three of which are related to airfoil modification. The researchers exclusively chose the thickness-to-camber ratio to modify the airfoils. These studies indicate that proper airfoil modification can improve airfoil performance. One of the airfoil studies further investigates a small HAWT designed with the modified airfoil. The rest of the two studies are about improving the self-starting torque of Darrieus VAWT. These two studies investigate the impact of the roughness of the blade surface employed by embossing. One of the turbine studies chooses the rotor height as the only physical parameter for investigation.

The current research is different from these five studies. Rather than modifying airfoils, this study evaluates five different base airfoils from five different families to identify the best-performing one for optimizing the performance of the Darrieus VAWT. It optimizes the performance based on the turbine's physical parameters like chord length, hub radius, circular angle, and blade length. This study also explicitly establishes a mathematical relationship between the chord length-to-hub radius ratio and C_P. It expresses the relationship using both the polynomial relationship and the modified Avrami equation and compares the best fit among the two expressions.

Dabachi et al. [18] designed a floating-type, three-stage rotor VAWT using QBlade. The researchers validated experimental data with numerical analysis and Qblade simulation results. It exploits only one type of airfoil with a Re of 100,000. The study analyses the performance of the designed turbine based on the number of blades, solidity, aspect ratio, radius, and different heights. The study investigates the impacts of a handful of parameters on C_P and power. However, it investigated only one airfoil and did not establish any mathematical relationship between the design parameters and performance. It could simulate different orientations of blades rather than only the H-type rotor.

Dabachi et al. [19] designed a three-stage Darrieus H-type rotor with different radii using QBlade. The study aimed to solve the problem of starting a large turbine using multiple-stage rotors. The study used the DU 06-W-200 airfoil with Re of 100,000 for the design. It presents the aerodynamic performance of the turbine and concludes that the increase of radius reduces the C_P but improves the mechanical power while using three variable rotor radii. The study presents a detailed design of the overall turbine setup. The analysis could use some other airfoils for the optimization and establish a mathematical relationship between different staged rotors with C_P.

The Avrami equation is conventionally used to describe the phase transformation in material systems. However, research identifies the effective use of the equation to describe data beyond the exclusive thermodynamic process. Such areas are life science, physical and social science, failure analysis, pandemic study, market analysis, and so on [20]. The Avrami equation can significantly describe a Sigmoidal (S-shaped) pattern of the data set [21].

The literature review emphasizes the main features of recent optimization efforts for VAWT design. It also points out the opportunities for improvements by integrating additional design parameters, exploring a wider variety of airfoil families, and developing mathematical expressions that relate design parameters to the C_P.

3. Methodology

The study utilizes QBlade software to examine the impact of parameter changes on aerodynamic and electrical performance [22]. QBlade is an open-source simulation software that can perform analyses on both HAWT and VAWT [23].

It can produce performance curves including various parameters such as TSR, C_P, etc. [24-26].

C_P is a critical parameter of wind turbine performance [24-26]. It is a measure of how efficiently each airfoil converts wind energy into mechanical energy. Higher values indicate better performance. The parameter, which is a non-dimensional quantity, can be expressed mathematically below

$$C_P = \frac{P}{\frac{1}{2}\rho A V^3} \tag{1}$$

where, P is the actual power extracted from the wind, ρ is the density of air, and A is the swept area.

The TSR is defined as the ratio between the actual V and the angular velocity, where r is the rotor radius. The expression is as follows

$$TSR = \frac{\omega r}{V} \tag{2}$$

QBlade facilitates the design and virtual construction of turbines using any airfoil coordinate files. The study takes airfoil coordinate files from the airfoil tools website. Fig. 2 shows the step-by-step simulation procedure in QBlade. In the first step, the user needs the airfoil coordinate files, and then the tool takes the airfoil coordinates as the airfoil input.

In step 3, the XFoil analysis or airfoil analysis provides the airfoil performance based on C_L and C_D values [24-26]. Mathematically, the C_L is expressed as the ratio between the lift force and the kinetic energy of the wind per unit volume expressed as

$$C_L = \frac{F_L}{\frac{1}{2}\rho A V^2} \tag{3}$$

The expression for C_D is given as

$$C_D = \frac{2F_D}{\rho A V^2} \tag{4}$$

The QBlade can show the individual airfoil performance curves on various configurations in a limited range of attack angles. In step 4, the same analysis covers the 360° angle of attack, referred to as 360° AoA. The extrapolation can produce performance results for individual airfoils.

However, the comparison of performance could be more detailed after simulating the rotor performance. At stage 5, users can prepare the blade. The module can take input from different design parameters like chord length, circular angle, height, and pitch angle. There are a number of blade segments where the user gives numeric values to complete the design of a single blade. At stage 6, the tool performs the rotor performance simulation using the DMST method.

Here, the user configures the simulation conditions. The values are mainly for environmental conditions, along with some statistical parameters. At stage 7, users are to input turbine configurations like the number of blades, ground clearance, and tower height. At stage 8, the overall turbine simulation takes place.

Here, simulation parameters like V, number of time steps, simulation length in seconds, rotational speed (rpm), and TSR are the main configurable parameters. The final performance result comprises the torque production, rpm, C_P, and TSR. Fig. 2 shows the parameter flow in each module in the QBlade simulation stages. The study takes five airfoils; these are 'DU 06-W-200', 'E168 (12.45%)', 'NACA M3', 'S1046 17% (Danny Howell)', and 'SG6043'.

The simulation produces the C_P, TSR, and other performance-indicating parameters based on different physical parameters of turbines. Based on the comparison of performance, the study selects the best-performing airfoil with the optimized physical parameters to design and analyze a suitable turbine for a low V site.

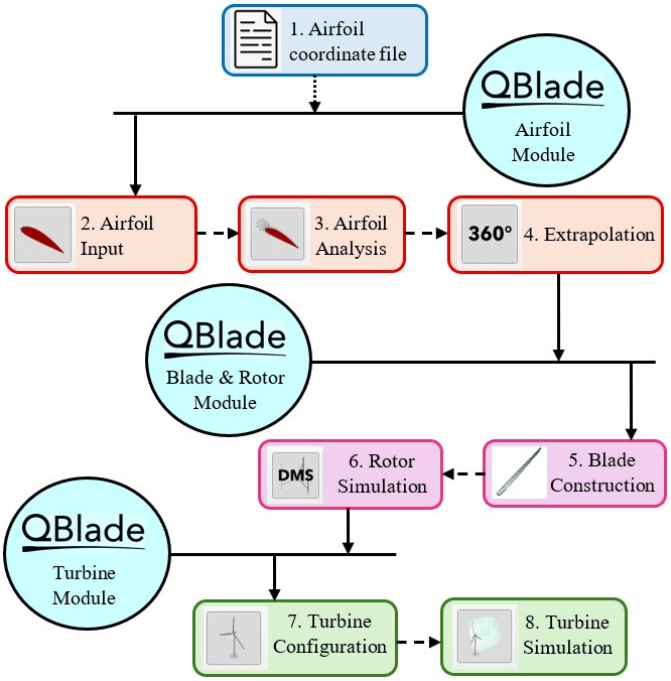

Fig. 2 Analysis flow

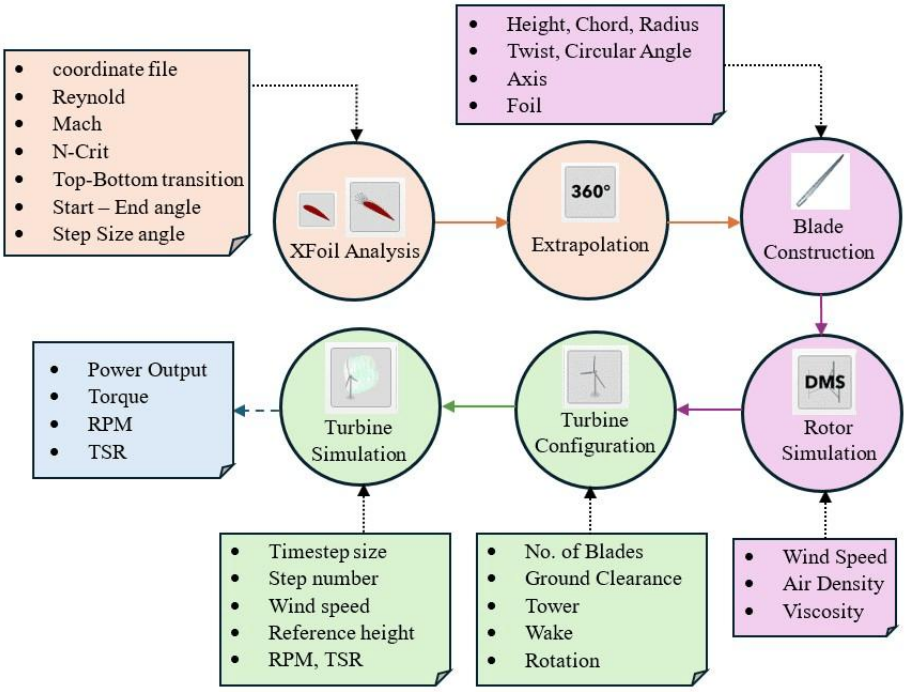

Fig. 3 Parameter flow of the simulation process

Fig. 3 presents the workflow of a wind turbine simulation process. It starts with XFoil Analysis, where aerodynamic characteristics are determined based on input parameters such as Re [24-26], Mach number, and airfoil coordinates. The results are then extrapolated to 360° for further analysis. Blade construction follows, incorporating parameters like height, chord, twist, and axis. The rotor simulation considers V, air density, and viscosity, while the turbine configuration defines structural parameters like the number of blades, tower, and wake effects. Finally, the turbine simulation calculates performance metrics such as torque, RPM, and TSR, providing insights into P.

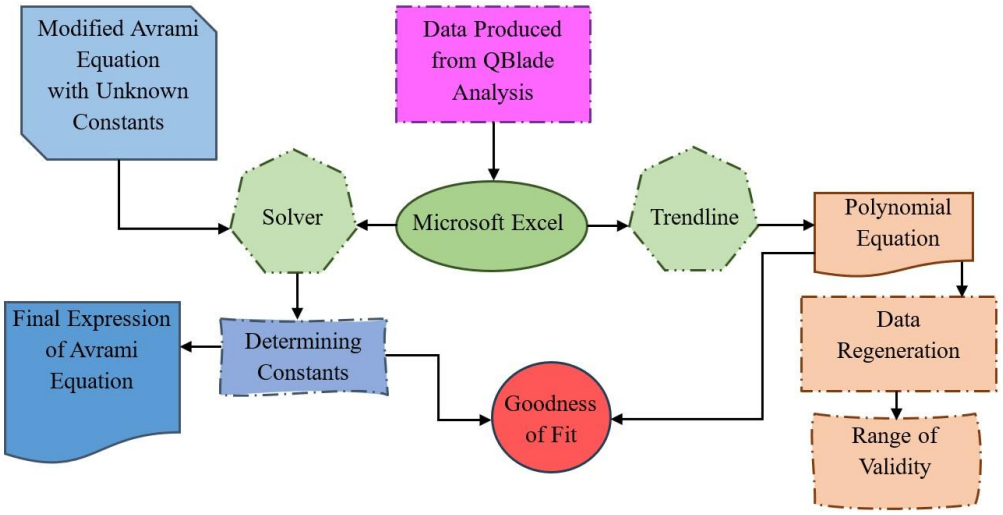

Fig. 4 Flow chart of mathematical expression preparation

Further, the study uses the data to establish a relationship between performance and design parameters like chord length and hub radius. For this, a mathematical expression is prepared using the Microsoft Excel program [27]. At first, the process fits data to the trendline using extrapolation and iterations, and then finds the goodness of fit using the R-Square value [28]. After that, the study finds the operational limit of the expression by regenerating data using the deduced equation. Along with this, the study uses a modified Avrami equation to find an optimized expression. Here, the process uses the Excel Solver program. Fig. 4 shows the two individual processes of preparing the polynomial equation and the Avrami equation.

The expression of the Avrami equation [29-30] can be expressed as:

$$f(t) = 1 - e^{-kt^n} \tag{5}$$

And the modified Avrami equation can be expressed as:

$$f(X) = G(1 - e^{-MX^T}) \tag{6}$$

where, G, M, and T are the constants. The study finds the best-fit values of these equation parameters. The study finds the extrapolated data's R-squared value to evaluate the goodness of fit. The Expression for R^2 is as follows.

$$R^2 = 1 - \frac{\sum (y_a - y_p)^2}{\sum (y_a - y_m)^2} \tag{7}$$

where, Y_a is the actual value, Y_P is the predicted value by the equation, and Y_m is the mean of the actual data. First, the study investigates the performance relationship using chord length and hub radius. Then, it uses three airfoils to further analyze circular angles and their impact on performance.

4. Analysis and Results

Among the five airfoils, DU 06-W-200, E168 (12.45%), NACA M3, and S1046 (17%) are symmetrical airfoils, as shown in Fig. 5. They are represented by red, green, black, pink, and blue colored lines, respectively. The DU 06-W-200 is commonly used for small VAWTs. In the case of the E168 (12.45%), it is an airfoil for working in low Re. The S1046 17% (Danny Howell) airfoil has a maximum thickness. Among these four airfoils, the NACA M3 is the thinnest, and except for the DU 06-W-200, the rest of the airfoils do not have any camber.

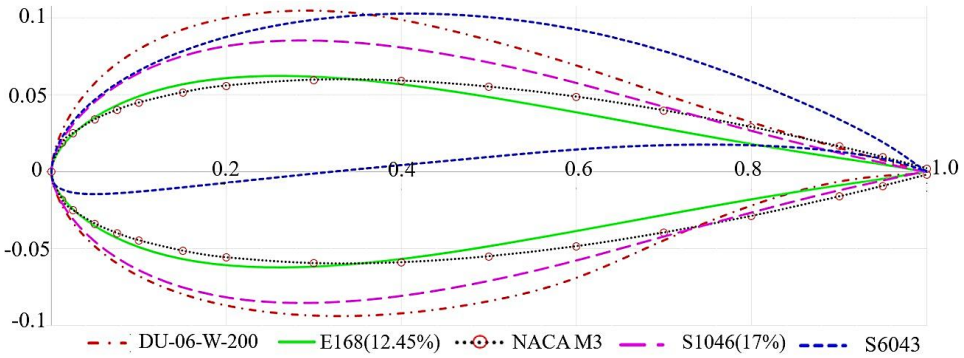

Fig. 5 Geometry of selected airfoils

The SG6043, represented by a blue colored line, is the only airfoil in this group with an asymmetrical shape. It is a widely used wind turbine airfoil with a high C_L/C_D. The QBlade program simulates and produces the aerodynamic performances of these airfoils.

4.1. Airfoil polar analysis

The graphs in Fig. 6 are polar graphs. Here, different parameters are observed over -20° to +20° AoA, denoted as "alpha." Fig. 6 (a) depicts the relationship between C_L and C_D, while Fig. 6 (b) relates the ratio of C_L over C_D. Fig. 7 (a) and 7 (b) show the relation of C_L and C_D to the AoA. It represents the efficiency of the airfoils by showing the C_L/C_D for a specific range of angles of attack.

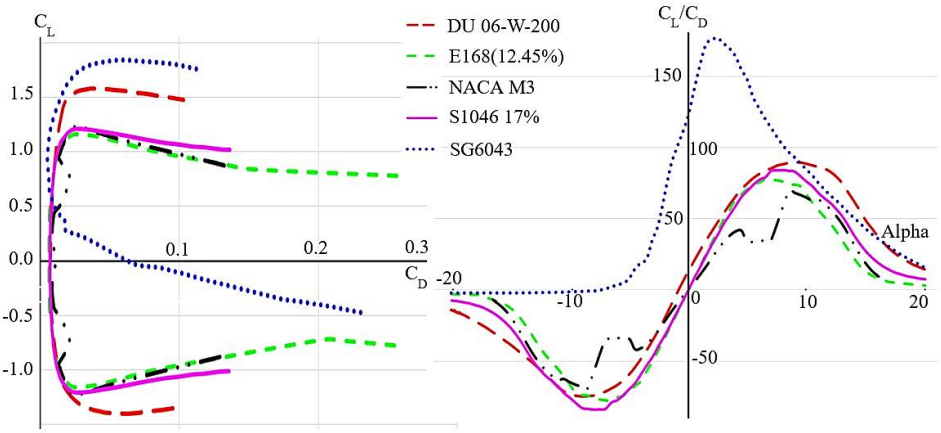

(a) C_L vs C_D (b) C_L/C_D vs. AoA

Fig. 6 Performance of C_L and C_D

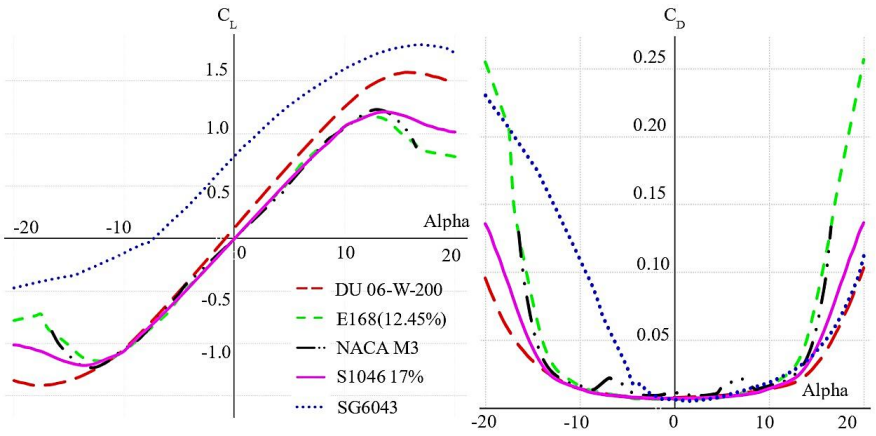

(a) C_L vs AoA (b) C_D vs AoA

Fig. 7 C_L and C_D vs AoA

Here, the DU 06-W-200 airfoil shows the best performance with a high and smooth lift line over a broad range of angles of attack, and it has a lower drag value, causing it to have a C_L/C_D of 89.94 and -74.92 at +9° and -9° of AoA, respectively. It also shows a higher amount of lift for different drag values by producing a uniform graph over the positive and negative AoA range, showing that it can harness the wind power from a more extensive range of directions. In addition, the SG6043 airfoil also shows this behavior, similar to the DU 06-W-200. A lower AoA can even suppress the DU 06-W-200 in the case of C_L/C_D and C_L. However, it does not produce a uniform graph, which is ill-suited for VAWTs, as in these wind energy harnessing devices, it is very common to face wind from any direction. Though it can achieve the highest amount of C_L/C_D at a lower AoA, even at 0° of AoA, having a C_L/C_D of 122.277, which is higher than that of any other airfoil mentioned in this study at that AoA, it will eventually be slowed down by the wind attacking at an angle of -5° or below.

On the other hand, the E168 (12.45%) and the S1046 17% (Danny Howell) show a similar pattern where the S1046 can utilize the wind to produce a lift force better than the E168. The E168 (12.45%) shows a lower amount of lift in high drag conditions, which contributes to the lower efficiency of that airfoil. Lastly, the NACA M3 airfoil shows a similar pattern to the previous two airfoils, but it also shows some fluctuations. The fluctuation is likely due to laminar-to-turbulent transition and flow separation, which results in complex flow behavior over the surface of the airfoil, causing instability and, thus, lower efficiency.

4.2. Extrapolation over 360°

QBlade simulates the airfoil performance over a 360° AoA. Figs. 8, 9, and 10 give the results of the 360° extrapolation. Here, the aerodynamic data of an airfoil is extended beyond the typical operating range to cover the full 360° range. This range is taken for VAWT as it encounters wind from all directions. All the lines level off at a C_L of around zero near ± 90° as flow separation occurs due to the edge-on to the flow position of the airfoils and near the exact value of the AoA; airfoils experience the maximum drag.

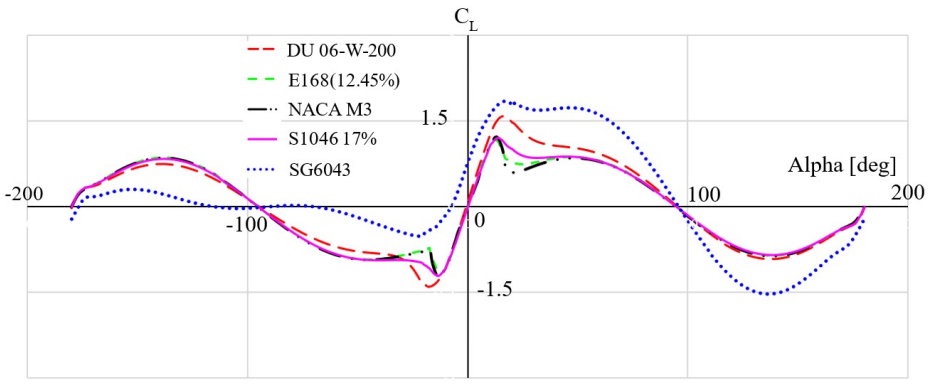

Fig. 8 360° extrapolation result on C_L

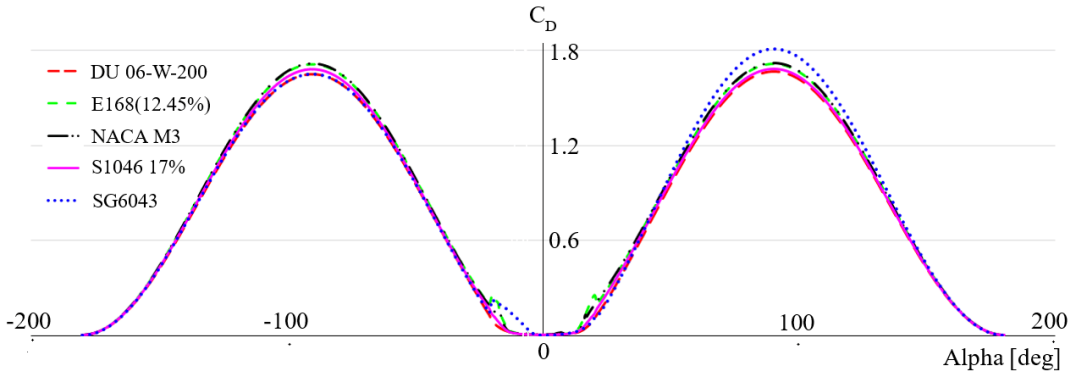

Fig. 9 360° extrapolation result on C_L, C_D, and C_L/C_D

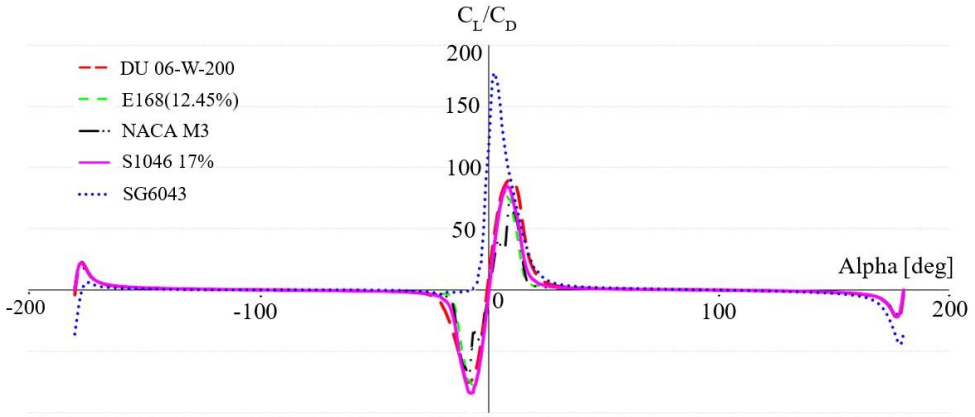

Fig. 10 360° extrapolation result on C_L/C_D

All the airfoils, except the NACA M3, show a smooth pattern, indicating that these are mainly suitable for a wide range of angles of attack. Moreover, the NACA M3 shows a higher drag value than others over a wide range of AoA. Though the SG6043 performs better than other airfoils within an AoA range of approximately -2° to 9°, peaking in C_L at around +5°, the DU 06-W-200, the S1046 17%, and E168 (12.45%) perform consistently at positive and negative angles of attack, resulting into a smooth usage of wind energy from a broader area to spin the turbine.

4.3. DMST results

By using the combinations of different chord lengths (0.01 m, 0.025 m, 0.05 m, 0.075 m, and 0.1 m) and various hub radii (0.5 m, 0.75 m, and 1 m), 15 '3-bladed' turbines with blades made from the subjected airfoils with a rotor height of 1.2 m were analyzed. The study observes the optimum TSR to generate maximum C_P, and thus, the C_P versus TSR graph was generated for all of the rotors. As shown in Fig. 11 (a), rotors with a chord length of 0.1 m and a hub radius of 0.5 m exhibit nearly identical performance across all combinations. The blades were analyzed up to a maximum TSR of 15. Among the five blades, the one made from the E168 (12.45%) and the S1046 17% show a positive C_P across an extensive range of TSR, which means that these two will be able to generate positive C_P within a more extensive range of blade speed-to-V ratio. On the other hand, the SG6043 can operate within a lower TSR range, as it achieves negative C_P at a TSR value of around 2.5, meaning that beyond that value of TSR, it will work as a fan rather than as a turbine.

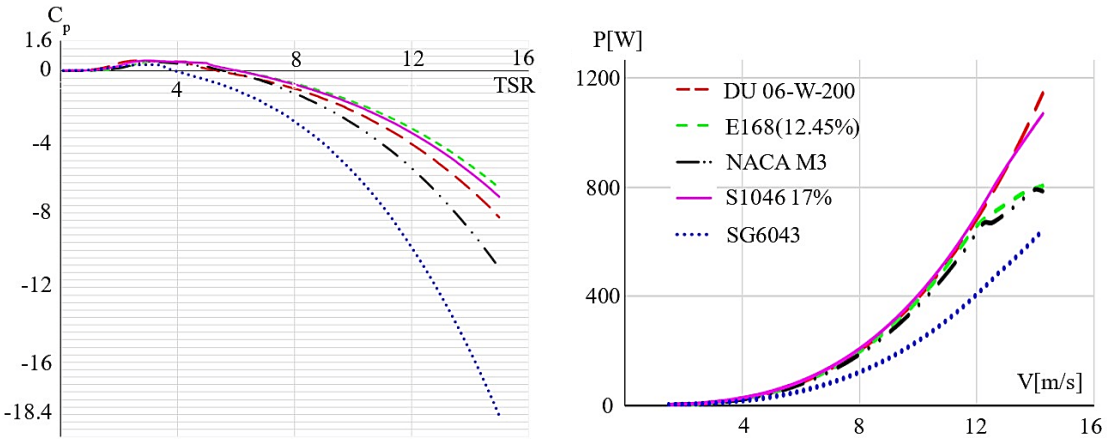

(a) C_P vs TSR (b) Power Curve vs V

Fig. 11 C_P and Power Curve of the Turbines

However, the DU 06-W-200 and the NACA M3 show a moderate range of TSR, which is slightly lower than that of the E168 (12.45%) and the S1046 (17%). Fig. 11 (b) represents the P in watts and V in m/s for various blades with a combination of a chord length of 0.1 m and a hub radius of 0.5 m. A similar trend is observed in all of the combinations. P mainly increases because of the V, as the power is proportional to the cube of the V. At lower V up to around 13 m/s, the S1046 17% blades

show the maximum output, which is overtaken by the P of the DU 06-W-200 blades after that speed. On the contrary, the SG6043 shows the lowest P, reaching only above 600 watts at 14 m/s, whereas the DU 06-W-200 outputs nearly 1100 watts at that speed. The E168 (12.45%) and the NACA M3 show almost similar patterns and produce about 800 watts for a V of 14 m/s, where the former blades produce slightly more power than the latter ones. However, the NACA M3 shows disturbance, and thus, the P gets lowered at around 13 m/s and 14 m/s.

5. Optimization and Parameter Relation

The study finds the optimized parameter configuration of chord length and hub radius by comparing the best-performing airfoil. Fig. 8 shows the trends of C_P over the change in chord length. Three hub radius values are investigated for a particular chord length, resulting in a total of 15 performance curves, as shown in Fig. 12. The S1046 airfoil shows the best performance in terms of C_P, where the optimized configuration of chord length is around 0.04 m, and the hub radius is 0.5 m. Table 1 presents data on the C_P for different airfoils at various circular angles. The angle started with 0° and gradually increased with the difference of 15°.

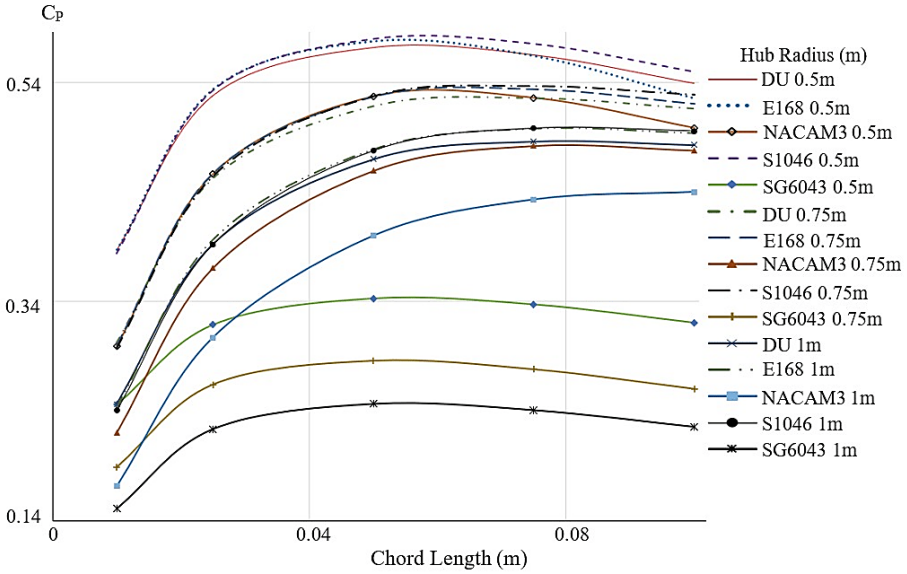

Fig. 12 Peak C_P vs. Chord Length

Table 1 C_P on varying Circular Angle

Type of Airfoils→ Circular Angle↓	C_P		
	DU 06-W-200	NACA M3	SG6043
0°	0.499410	0.456351	0.246718
15°	0.499411	0.456351	0.246726
30°	0.499410	0.456351	0.246717
45°	0.499413	0.456351	0.246747
60°	0.499407	0.456351	0.246681
75°	0.499413	0.456351	0.246751
90°	0.499410	0.456351	0.246720
	Highest C_P at TSR- 3.8	Highest C_P at TSR- 3.6	Highest C_P at TSR- 3.7

Here, the table compares three airfoil types: DU 06-W-200, NACA M3, and SG6043. The circular angles at which the blades are positioned relative to the wind range from 0° to 90° in increments of 15°. However, the performance does not vary much with the variation of the circular angle. All the airfoils maintain their respective highest C_P value across all angles. The DU 06-W-200 has a C_P value of around 0.4994, the NACA M3 reaches 0.4563, while the SG6043 airfoil has significantly lower C_P values, around 0.2467, making it the least efficient of the three. On the other hand, the DU 06-W-200 shows the highest C_P among these three airfoils. In every case, the DU 06-W-200 shows the best performance at 3.8 TSR, while the NACA M3 and the SG6043 show it at 3.6 TSR and 3.7 TSR, respectively.

Since the circular angle has a negligible impact on improving the performance of the turbine prepared using the selected airfoils, the study selects chord length and hub radius to develop a relationship between optimization parameters and performance indicators, i.e., C_P and TSR.

5.1. Polynomial expression of performance

The analysis investigates the C_P over various chord lengths and hub radii. Due to the ease of combining these two variables, the analysis takes the ratio between chord length and hub radius. Fig. 13 (a) shows the trends of maximum C_P, and Fig. 13 (b) shows the usable TSR based on the change in chord length and hub radius. Since the best performance data was gathered for the S1046 airfoil, an equation using the data of the S1046 airfoil is produced. The polynomial line tends to follow Eq. (8) for C_P and the logarithmic trend by Eq. (9) for TSR. The goodness of fit (R^2) for C_P line 0.9485 (94.85%) and 0.9938 (99.38%) for TSR. The term x represents the chord length to hub radius ratio, and y represents the C_P and TSR.

$$y = 19969x^5 - 1311x^4 + 3236.6x^3 - 374.08x^2 + 20.677x + 0.0768 \quad (8)$$

$$y = -2.419\ln(x) - 1.3671 \quad (9)$$

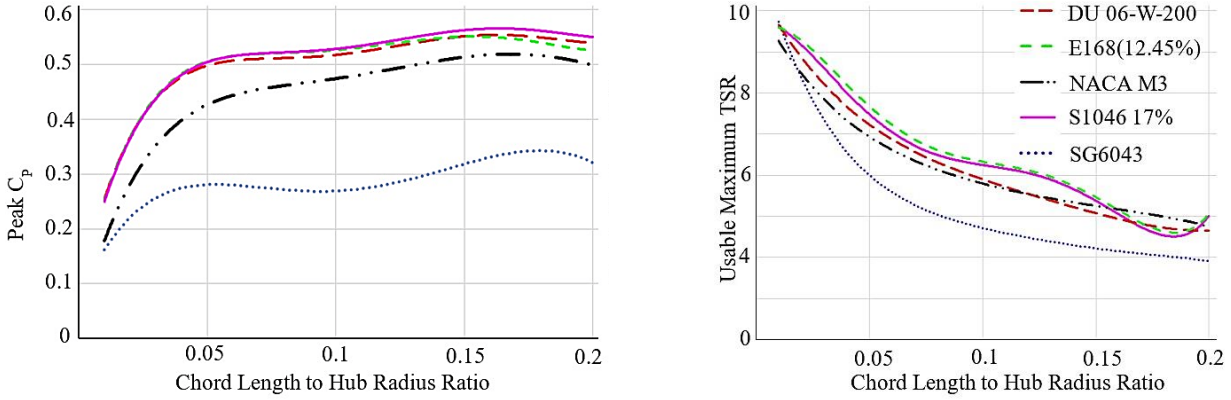

(a) Peak C_P (b) Usable TSR

Fig. 13 Performance based on different Chord length to Hub Radius ratio

Eq. (8) has a total of 6 terms with a constant of 0.0768. Eq. (9) has only two terms with a constant of -1.3671. The goodness of fit for both equations is quite good; however, the number of terms is a handful for Eq. (8), and the goodness of fit is lower than for Eq. (9). Fig. 14 shows the regenerated performance data by Eq. (8). It is found that the C_P exceeds Betz's limit after the ratio of around 0.23. So, the relationship is not sustained after this range since C_P cannot be more than 59.3% (0.593). However, the equation is valid within a range of 0 < Ratio < 0.23.

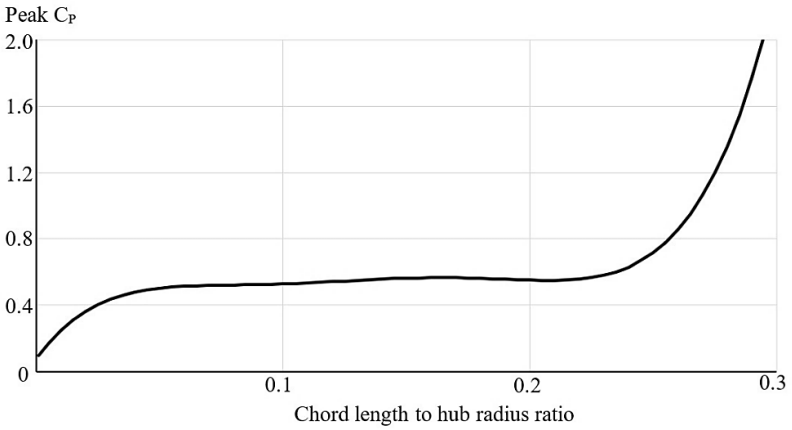

Fig. 14 Regeneration of data using the polynomial equation

5.2. Expression of performance using the Avrami equation

It is observed that the C_P versus the chord length to hub radius ratio data somewhat resembles an 'S' shape. The Avrami equation can significantly fit the S-shaped data population. The modified Avrami equation given as Eq. (6) is used to extrapolate the data. In the equation, three unknowns, G, M, and T, are computed using the 'Microsoft Excel Solver' module. Fig. 15 shows the curve fitting between the original data and the extrapolated data. The solid line shows the original data, and the dotted line shows the extrapolated data. The figure consists of four airfoil curves fitting identified by the airfoil names in the top tag lines.

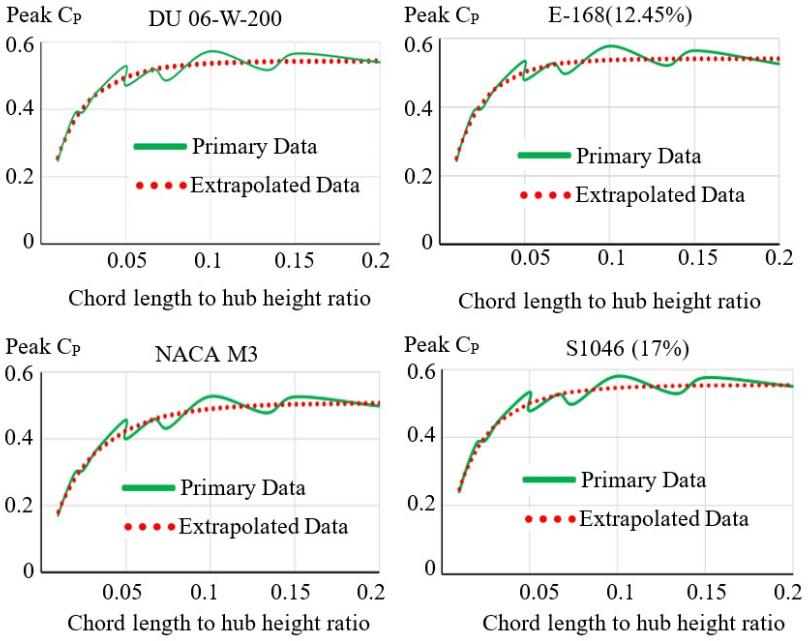

Fig. 15 Extrapolation using the modified Avrami equation

Table 2 gives the estimated values for the unknown quantities of the modified Avrami equation for different airfoils. It also gives the goodness of fit (R^2) for each curve. The highest goodness of fit is observed for the data of the NACA airfoil. The goodness of fit is improved by using a modified Avrami equation by 1% to that of polynomial extrapolation.

Table 2 Parameter values of the modified Avrami equation and goodness of fit

Airfoils	G	M	T	R^2
DU	0.54	29.45	0.83	94.8%
E-168	0.54	39.78	0.90	95.36%
NACA	0.51	25.38	0.88	96.24%
S1046	0.55	29.90	0.85	95.87%

5.3. Performance of the optimized turbine by variant

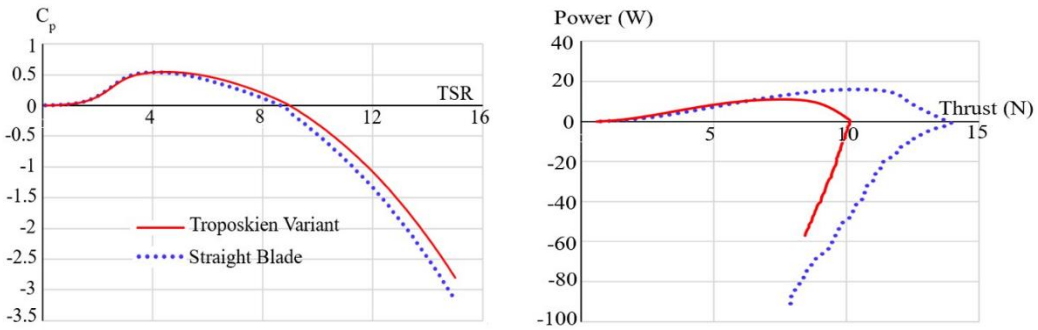

(a) C_P Vs TSR (b) Power Vs Thrust

Fig. 16 Performance by turbine variants

The optimized 3-bladed simple VAWT made from the S1046 17% airfoil with a rotor height of 1.2m, a chord length of 0.075 m, and a hub radius of 0.75m is further checked for performance by variants. The straight-bladed turbine performance is compared with the Troposkien variant, as shown in Figs. 16 (a) and 16 (b). The straight-bladed turbine shows comparatively higher peak P (15.9308 watts) at a higher thrust (10.448N), while the Troposkien has a peak P of 11.142 watts at a thrust of 7.61093N. It also has a lower peak thrust of 10.1491N, whereas the other turbines show 13.9757N. However, at peak thrust, only the Troposkien shows a positive P of 0.406624 watts. Other turbines show positive P with a thrust value of 13.778N (straight-bladed turbine). Among these turbines, the Troposkien turbine shows the best result, with a maximum C_P of 0.547073 at a TSR of 4.5.

On the other hand, all other turbines in this group reach their maximum C_P at a TSR of 4.1, showing a similar value of 0.536192. A similar trend can be seen regarding the maximum usable TSR, where the Troposkien shows positive C_P until 8.9 TSR, and the rest of the turbines limit themselves to 8.6. Therefore, the Troposkien turbine converts more energy positively at a higher V, unlike the others.

The results conclude that the Troposkien turbine is more efficient than the other variants as it has a higher C_P along with a higher usable TSR value. This means that it will generate more power at the optimum TSR compared to others and produce positive P throughout a higher range of TSR. The power versus thrust curve suggests that the straight-bladed and helix turbines exert more stress on the mechanisms of the turbine, unlike the Troposkien turbine, as higher thrust creates a bending moment on the structure. However, the Troposkien turbine produces less power at the same thrust, but as it is the most stable one, this will be in service with a lot less maintenance and energy spikes that will increase its service life.

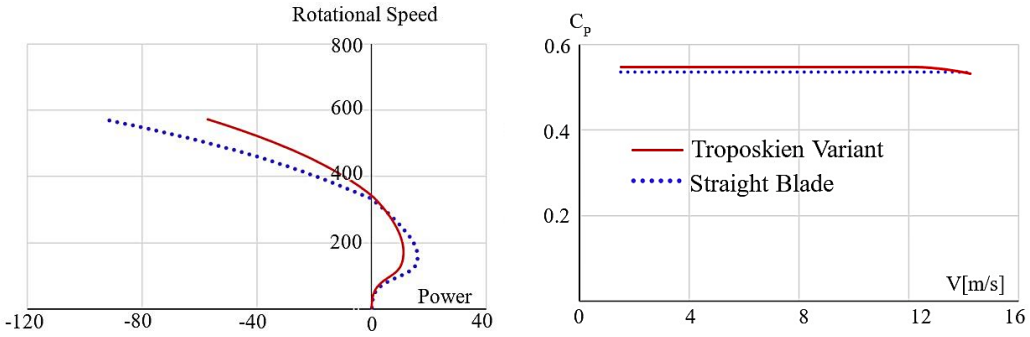

(a) Power by rotational speed (b) C_P vs V

Fig. 17 Performance by turbine variants

In the case of the relation between the rotational speed of the turbine and power as given in Fig. 17 (a), the highest values of power obtained from the turbines are 11.142 watts at 171.887 rpm for the Troposkien turbine, and 15.9308 watts at 156.608 rpm for all other turbines. However, the Troposkien can generate positive power up to a higher rpm of 339.955, primarily due to its higher value of usable TSR, where all the other turbines cap at 328.496 rpm. From the C_P vs. V curve in Fig. 17 (b), the Troposkien turbine reaches its maximum C_P (0.547073) at a relatively lower V (12 m/s), whereas every other turbine in the group works at the same maximum C_P of 0.536224 at a V of 13.5 m/s. This result shows that the Troposkien turbine can generate more power at a lower V. Further increase of the V causes the C_P to fall from these points.

However, the power versus V diagram does not favor the Troposkien turbine. While the straight-blade variant generates 15.9308 watts of power at 3 m/s of V, this one can only generate 11.142 watts, as shown in Fig. 18. This lower power can be due to the turbine's smaller surface area compared to the straight-bladed turbine.

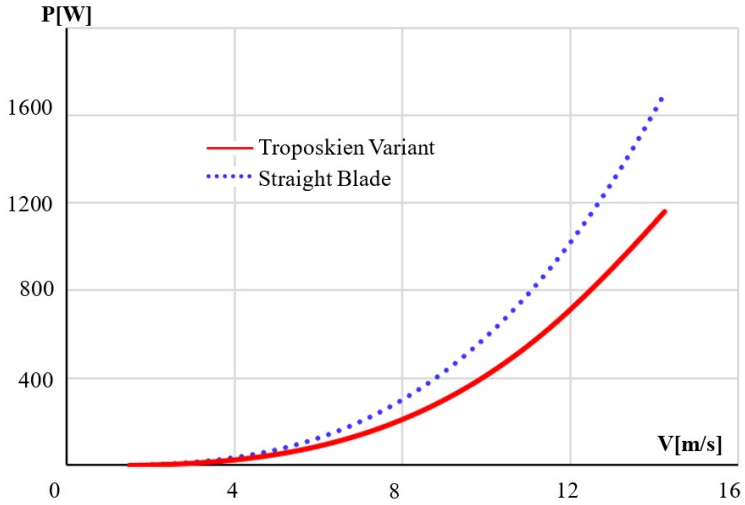

Fig. 18 Performance by turbine variants

6. Conclusions

This research investigates five airfoils to identify the suitable airfoil for a small VAWT while optimizing chord length, hub radius, and circular angle using QBlade software. The study identifies the chord length and hub radius as the most influential parameters, with the circular angle having minimal impact on efficiency. Two mathematical models were developed to describe the performance based on the optimizing parameters. One is the six-term polynomial expression, and another is the modified Avrami equation. From the design standpoint, the Troposkien blade variant demonstrates better performance across a broader range of V, while the straight blade is good for higher P. The key outcomes are given below:

(1) The optimization uses Chord Length, Hub Radius, and Circular angle to design a small VAWT.

(2) Upon optimization of the chord length and hub radius, the circular angle has a negligible impact on performance.

(3) The optimized chord length is 0.04 m, and the Hub Radius is 0.5 m.

(4) The best-performing airfoil is S1046 (17%) (Danny Howell), resulting in the highest C_P 56% and TSR 9.8

(5) The polynomial relation gives a six-term expression and fits the performance data by 94%, and the modified Avrami equation provides a concise expression with only three terms and a 95% goodness of fit.

(6) The polynomial expression remains valid within the chord length to hub radius ratio range of 0 to 2.25.

(7) The expression can provide a generalized relation of performance over-optimization for small VAWTs, which would contribute to the design and development of efficient wind turbines.

(8) The Troposkien variant of the optimized turbine is more suitable because it offers a broader range of improved C_P across a wide range of V values.

(9) The straight blade variant could be used for a higher P than the Troposkien variant.

Acknowledgments

This study was supported by the Institute of Energy, University of Dhaka, and partly funded by the American International University-Bangladesh (AIUB).

Conflicts of Interest

The authors declare no conflict of interest.

References

[1] T. Z. Ang, M. Salem, M. Kamarol, H. S. Das, M. A. Nazari, and N. Prabaharan, "A Comprehensive Study of Renewable Energy Sources: Classifications, Challenges and Suggestions," Energy Strategy Reviews, vol. 43, article no. 100939, 2022.

[2] P. Muthukumar, D. K. Sarkar, D. De, and C. K. De, Innovations in Sustainable Energy and Technology, 1st ed., Singapore, Springer Singapore, 2021.
[3] M. Hasan, P. Dey, S. Janefar, N. A. Salsabil, I. J. Khan, N. R. Chowdhury, et al., "A Critical Analysis of Wind Energy Generation Potential in Different Regions of Bangladesh," Energy Reports, vol. 11, pp. 2152-2173, 2024.
[4] H. Muhsen, W. Al-Kouz, and W. Khan, "Small Wind Turbine Blade Design and Optimization," Symmetry, vol. 12, no. 1, article no. 18, 2019.
[5] A. I. Altmimi, A. Aws, M. J. Jweeg, A. M. Abed, and O. I. Abdullah, "An Investigation of Design and Simulation of Horizontal Axis Wind Turbine Using QBlade," Measurement Science Review, vol. 22, no. 6, pp. 253-260, 2022.
[6] M. R. Badah and Y. H. Mahmood, "Performance Analysis of Vertical Axis Wind Turbine Blades Using Double Multiple Stream Tube Process," Iraqi Journal of Science, vol. 63, no. 8, pp. 3366-3372, 2022.
[7] A. I. Altmimi, M. Alaskari, O. I. Abdullah, A. Alhamadani, and J. S. Sherza, "Design and Optimization of Vertical Axis Wind Turbines Using QBlade," Applied System Innovation, vol. 4, no. 4, article no. 74, 2021.
[8] A. Muratoğlu and M. S. Demir, "Investigating the Effect of Geometrical and Dynamic Parameters on the Performance of Darrieus Turbines: A Numerical Optimization Approach via QBlade Algorithm," Bitlis Eren Üniversitesi Fen Bilimleri Dergisi, vol. 9, no. 1, pp. 413-426, 2020.
[9] K. Deghoum, M. T. Gherbi, H. S. Sultan, A. N. Jameel Al-Tamimi, A. M. Abed, O. I. Abudullah, et al., "Optimization of Small Horizontal Axis Wind Turbines Based on Aerodynamic, Steady-State, and Dynamic Analyses," Applied System Innovation, vol. 6, no. 2, article no. 33, 2023.
[10] F. Ardaneh, A. Abdolahifar, and S. M. H. Karimian, "Numerical Analysis of the Pitch Angle Effect on the Performance Improvement and Flow Characteristics of the 3-PB Darrieus Vertical Axis Wind Turbine," Energy, vol. 239, Part D, article no. 122339, 2022.
[11] L. Merad, A. Bouanani, and M. Bouchaour, "Modeling and Simulation of the Vertical Axis Wind Turbine by QBlade Software," Algerian Journal of Renewable Energy and Sustainable Development, vol. 2, no. 2, pp. 181-188, 2020.
[12] H. Zhang, Y. Hu, and W. Wang, "Wind Tunnel Experimental Study on the Aerodynamic Characteristics of Straight-Bladed Vertical Axis Wind Turbine," International Journal of Sustainable Energy, vol. 43, no. 1, article no. 2305035, 2024.
[13] H. S. Davari, R. M. Botez, M. S. Davari, H. Chowdhury, and H. Hosseinzadeh, "Numerical and Experimental Investigation of Darrieus Vertical Axis Wind Turbines to Enhance Self-Starting at Low Wind Speeds," Results in Engineering, vol. 24, article no. 103240, 2024.
[14] H. S. Davari, R. M. Botez, M. S. Davari, H. Chowdhury, and H. Hosseinzadeh, "Blade Height Impact on Self-Starting Torque for Darrieus Vertical Axis Wind Turbines," Energy Conversion and Management: X, vol. 24, article no. 100814, 2024.
[15] H. S. Davari, M. S. Davari, S. Kouravand, and M. K. Kurdkandi, "Optimizing the Aerodynamic Efficiency of Different Airfoils by Altering Their Geometry at Low Reynolds Numbers," Arabian Journal for Science and Engineering, vol. 49, pp. 15253-15288, 2024.
[16] H. S. Davari, R. M. Botez, M. S. Davari, and H. Chowdhury, "Enhancing Aerodynamic Efficiency: Shape Modification of Airfoils," International Journal of Ambient Energy, vol. 45, no. 1, article no. 2439441, 2024.
[17] H. S. Davari, M. S. Davari, R. M. Botez, and H. Chowdhury, "Maximizing the Peak Lift-to-Drag Coefficient Ratio of Airfoils by Optimizing the Ratio of Thickness to the Camber of Airfoils," Sustainable Earth Review, vol. 3, no. 4, pp. 46-61, 2023.
[18] M. A. Dabachi, A. Rahmouni, E. Rusu, and O. Bouksour, "Aerodynamic Simulations for Floating Darrieus-Type Wind Turbines with Three-Stage Rotors," Inventions, vol. 5, no. 2, article no. 18, 2020.
[19] M. A. Dabachi, A. Rahmouni, O. Bouksour, "Design and Aerodynamic Performance of New Floating H-Darrieus Vertical Axis Wind Turbines," Materials Today: Proceedings, vol. 30, no. 4, pp. 899-904, 2020.
[20] K. Shirzad and C. Viney, "A Critical Review on Applications of the Avrami Equation Beyond Materials Science," Journal of the Royal Society Interface, vol. 20, article no. 203, 2023.
[21] B. Cantor, The Equations of Materials, 1st ed., Oxford University Press, 2020.
[22] L. S. Wang, W. Cao, and S. Hu, Entropy and Exergy in Renewable Energy, 1st ed., IntechOpen, 2022.
[23] R. A. Khaddar, S. K. Singh, N. D. Kaushika, R. K. Tomar, and S. K. Jain, Recent Developments in Energy and Environmental Engineering, Lecture Notes in Civil Engineering, 1st ed., Springer Nature Singapore, 2023.
[24] H. S. Davari, R. M. Botez, M. S. Davari, and H. Chowdhury, "Enhancing the Efficiency of Horizontal Axis Wind Turbines Through Optimization of Blade Parameters," Journal of Engineering, vol. 2024, no. 1, article no. 8574868, 2024.

[25] H. S. Davari, S. Kouravand, M. S. Davari, and Z. Kamalnejad, "Numerical Investigation and Aerodynamic Simulation of Darrieus H-rotor Wind Turbine at Low Reynolds Numbers," Energy Sources Part A: Recovery, Utilization, and Environmental Effects, vol. 45, no. 3, pp. 6813-6833, 2023.

[26] H. S. Davari, M. S. Davari, R. M. Botez, and H. Chowdhury, "Advancements in Vertical Axis Wind Turbine Technologies: A Comprehensive Review," Arabian Journal of Science and Engineering, vol. 50, no. 4, pp. 2169-2216, 2025.

[27] A. Wongphat, S. Wongcharee, N. Chaiduangsri, K. Suwannahong, T. Kreetachat, S. Imman, et al., "Using Excel Solver's Parameter Function in Predicting and Interpretation for Kinetic Adsorption Model via Batch Sorption: Selection and Statistical Analysis for Basic Dye Removal onto a Novel Magnetic Nanosorbent," ChemEngineering, vol. 8, no. 3, article no. 58, 2024.

[28] C. Onyutha, "A Hydrological Model Skill Score and Revised R-Squared," Hydrology Research, vol. 53, no. 1, pp. 51-64, 2021.

[29] B. Cantor, The Equations of Materials, The Avrami Equation: Phase Transformations, Oxford Academic, 2020.

[30] A. Bishay, Recent Advances in Science and Technology of Materials, 1st ed., New York: Springer New York, 2012.